

Article

Control of Magnetic Properties of NiMn_2O_4 by a Microwave Magnetic Field under Air

Hiroshi Goto, Jun Fukushima * and Hirotsugu Takizawa

Department of Applied Chemistry, Tohoku University, Aoba Aramaki, Sendai, Miyagi 980-8579, Japan; goto@aim.che.tohoku.ac.jp (H.G.); takizawa@aim.che.tohoku.ac.jp (H.T.)

* Correspondence: fukushima@aim.che.tohoku.ac.jp; Tel.: +81-22-795-7226

Academic Editor: Dinesh Agrawal

Received: 29 December 2015; Accepted: 24 February 2016; Published: 4 March 2016

Abstract: NiMn_2O_4 prepared by conventional heating was irradiated with a microwave H-field using a single-mode cavity under air and magnetic properties of the microwave-irradiated material were investigated. X-ray diffraction and transmission electron microscopy demonstrated that the phase and microstructure are not affected by H-field irradiation. Measurements of the magnetization as a function of temperature revealed that the antiferromagnetic sublattice disappeared and electron spin resonance showed the existence of Mn^{2+} , suggesting that Mn^{3+} is partially reduced. Moreover, the magnetization of NiMn_2O_4 was controlled from 35.3 to 18.2 emu/g and the coercivity from 140 to 750 Oe by changing the sample temperature during microwave irradiation. The reduction reaction of NiMn_2O_4 is controlled by microwave H-field irradiation, resulting in control over the magnetic properties.

Keywords: microwave H-field irradiation; manganese spinel oxides; reduction reaction

1. Introduction

Valence control in transition-metal-containing materials is used for obtaining desired functional (e.g., conducting, magnetic, and superconducting) materials, and it can be achieved through doping, oxidation, and reduction reactions. Examples of valence control by changing oxygen stoichiometry are the syntheses of SrFeO_2 and $\text{Sr}_3\text{Fe}_2\text{O}_5$ (which have abnormal Fe valences) [1,2] by reduction with CaH_2 , [3–5] the synthesis of $\text{YBa}_2\text{Cu}_3\text{O}_{7-x}$ [6], LaMnO_3 [7], and $\text{La}_{1-x}\text{Sr}_x\text{FeO}_{3-x}$ [8] at high temperatures under reducing atmospheres, and the synthesis of MnCo_2O_4 by atomic layer deposition [9]. These techniques require the use of a metal hydride that is highly moisture-sensitive, a controlled atmosphere (hydrogen gas), or a special device, respectively.

Nickel manganite (NiMn_2O_4) is an essential application material for negative-temperature-coefficient (NTC) thermistors [10], catalysts [11–13], and future spintronic devices [14,15]. Nickel manganite crystallizes in the spinel structure and manganese ions of several valences (Mn^{2+} , Mn^{3+} , and Mn^{4+}) are assigned to the tetrahedral and octahedral sites. The magnetic properties of nickel manganite can be controlled by reduction, thereby changing the valences of manganese ions. Nonstoichiometric $\text{NiMn}_2\text{O}_{4-x}$ has a complex magnetic structure (ferrimagnetic-like), which is produced by the competition between antiferromagnetic and ferromagnetic sublattices [16,17].

Reduction reactions proceed more rapidly with microwave irradiation than with conventional heating under the same atmosphere and at the same temperature [18,19]. In a microwave process, when the material's temperature is steady, the material is in a nonequilibrium steady state: microwave energy constantly enters the material, and absorbed energy is released as thermal energy by conduction, convection, and radiation. Thus, it is quite possible that unexplained reduction behavior by thermodynamics was observed [20]. Microwave processing is expected to be a simple

reduction process, because a controlled atmosphere is not required. In addition, the process has unique heating characteristics (internal heating, rapid heating, *etc.*), and it is expected to be applied to the refining of powders of iron oxide [21–23]. Microwave energy can be supplied directly to powders and the energy efficiency for the refining of powders with microwaves is higher than with a conventional gas-heating process. However, reduction by irradiation with microwaves has not received much scrutiny. Although changes in crystal structures, morphologies, magnetic properties and resistivity of iron-containing oxides, caused by microwave irradiation, have been reported [24–26], the effect for other transition-metal-containing oxides is unknown.

In this study, NiMn_2O_4 was irradiated with microwave H-field using a single-mode cavity and magnetic properties after microwave irradiation were investigated. In addition, the magnetic properties of NiMn_2O_4 were controlled by changing the microwave-irradiation conditions.

2. Experimental Section

2.1. Preparation of Single-Phase NiMn_2O_4

NiMn_2O_4 was prepared by a solid-state reaction. Stoichiometric amounts of NiO (>99.0%, Wako Pure Chem. Industries, Ltd., Tokyo, Japan) and MnCO_3 (>99.9%, Kojundo Chem. Lab. Co., Ltd., Saitama, Japan) were weighed so as to equal mole ratio and mixed using ethanol. After drying by thermostatic oven at 80 °C, the mixed powder was calcined at 850 °C for 12 h using an electric furnace (F0100, Yamato Scientific Co., Ltd., Tokyo, Japan). The sample was pressed into pellets with a diameter of 10 mm, which were sintered at 850 °C for 12 h. During sample sintering, the temperature in the electric furnace was measured with a thermocouple. The sample was reground and pressed into pellets of the same size, which were calcined under the same conditions. The sample is denoted as Pre- NiMn_2O_4 .

2.2. Microwave Irradiation of NiMn_2O_4 at the Maximum Point of Microwave H-Field Intensity

Presynthesized NiMn_2O_4 was reground and 0.3 g of it was pressed into a pellet with a diameter of 6 mm and a height of 2 mm. Figure 1 shows the setting of the microwave irradiation at the maximum point of microwave H-field intensity. The pellet was placed in a quartz glass tube and set in the TE102 cavity.

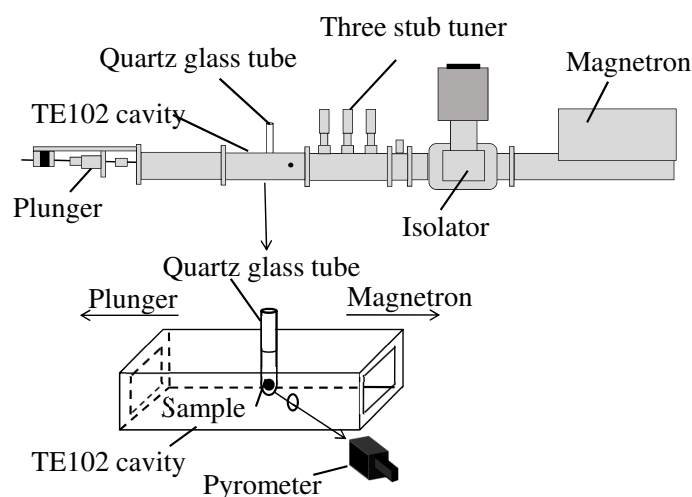


Figure 1. Schematic view of the microwave irradiation device and the sample setting of microwave irradiation at the maximum point of H-field intensity.

There is a standing wave in the TE102 cavity and the maximum point of microwave H-field or E-field intensity can be separated spatially. The sample was irradiated with microwave by a

magnetron (IMH-20A259, IDX Co., Ltd., Tochigi, Japan, 2455 ± 15 MHz). In this experiment, the NiMn_2O_4 pellet was set at the maximum point of microwave H-field intensity. The temperature of the sample was measured with a pyrometer (FTK9P300, Japan Sensor Co., Tokyo, Japan), which measure infrared radiation in the region of 1.95 to 2.5 μm , through a hole on the side of the TE102 cavity. The sample was inserted in a quartz tube, which has well transparency of the 1.95 to 2.5 μm light. The pellet was heated to 850 $^\circ\text{C}$ for 10 min with microwave irradiation. For comparison, another pellet of the same size was heated to 850 $^\circ\text{C}$ for 6 h using an electric furnace. After conventional heating, the sample was furnace-cooled.

To investigate whether oxygen vacancies in the H-field-irradiated sample cause the changes in the magnetic properties, the microwave-irradiated sample was reground, pelletized and annealed for oxidation with an electric furnace to 850 $^\circ\text{C}$ for 6 h in air.

Samples were characterized by X-ray diffraction (XRD, Rigaku, Tokyo, Japan, RINT-2000,) and field-emission scanning transmission electron microscopy (FE-STEM, Hitachi High-Technologies Corporation, Tokyo, Japan). Magnetic properties were characterized with a superconducting quantum interface device (SQUID, Tokyo, Japan, Quantum Design, MPMS-XL). The spin states of the samples were analyzed by electron spin resonance (ESR, JEOL RESONANCE, Tokyo, Japan, JES-X330). The samples measured by ESR were diluted to 15 wt % using $\alpha\text{-Al}_2\text{O}_3$ (99.9%, Rare Metallic Co., Ltd., Tokyo, Japan).

3. Results and Discussion

3.1. Phase and Microstructure after Microwave H-Field Irradiation

Reported experimental conditions for the synthesis of NiMn_2O_4 are ambiguous. Although previous work indicated the NiMn_2O_4 spinel phase was reported to be synthesized by quenching from 1100 $^\circ\text{C}$ [16], another paper reported the formation of another Ni-Mn-O phase around 1100 $^\circ\text{C}$ [27]. Therefore, we synthesized NiMn_2O_4 at 850 $^\circ\text{C}$ using a microwave or an electric furnace to prevent the sample from decomposing in this experiment. As shown in Figure 2, presynthesized NiMn_2O_4 consists of the spinel phase only.

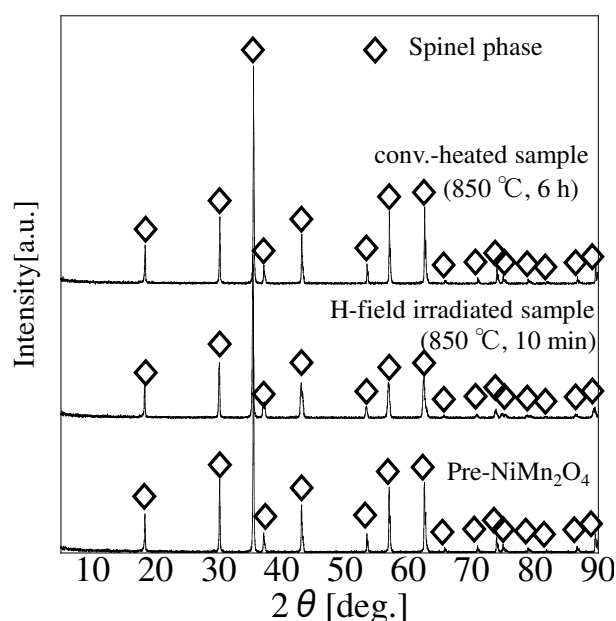


Figure 2. X-ray diffraction (XRD) patterns of synthesized NiMn_2O_4 .

Therefore, this sample (denoted by Pre-NiMn₂O₄) was used for microwave irradiation or electric-furnace heating. After microwave H-field irradiation (H-field-irradiated sample) or conventional heating (conv.-heated sample), all samples keep its phase and there is no other phase. Lattice constants of these samples not significant difference compared to that of Pre-NiMn₂O₄. As nickel manganite has various manganese ions state (Mn²⁺, Mn³⁺ and Mn⁴⁺) and the ions are assigned to the tetrahedral and octahedral sites, it is considered that the differences of lattice constants among these samples was not changed significantly. Consequently, pure NiMn₂O₄ spinel phase can be synthesized at 850 °C and NiMn₂O₄ is not decomposed by microwave or electric-furnace heating. The texture of the sample was not changed in the order of micrometer (Supplementary material 1). Figure 3 shows TEM images and electron-diffraction images.

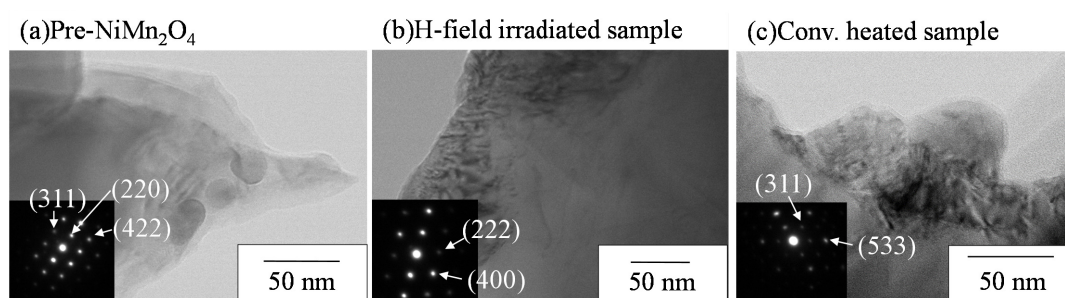


Figure 3. TEM images and electron-diffraction patterns of synthesized NiMn₂O₄. (a) Pre-NiMn₂O₄; (b) H-field irradiated sample; (c) Conv. heated sample.

Pre-NiMn₂O₄ and the H-field-irradiated sample have the same sharp diffraction images. Therefore, the microstructure of NiMn₂O₄ was not affected by microwave H-field irradiation. Previous paper has reported that the magnetism of Fe₃O₄ is changed through the formation of nanodomain structures [25]. Based on XRD and TEM images, there is no apparent difference between Pre-NiMn₂O₄ and the H-field-irradiated sample. Thus it is suggested that the interaction between NiMn₂O₄ and the microwave H-field is different from that between ferrite and the microwave H-field.

3.2. Magnetic Properties of H-Field-Irradiated NiMn₂O₄

Figure 4 shows M-H loops at 5 K and Table 1 shows the saturation magnetization and coercivity of NiMn₂O₄ obtained from Figure 4.

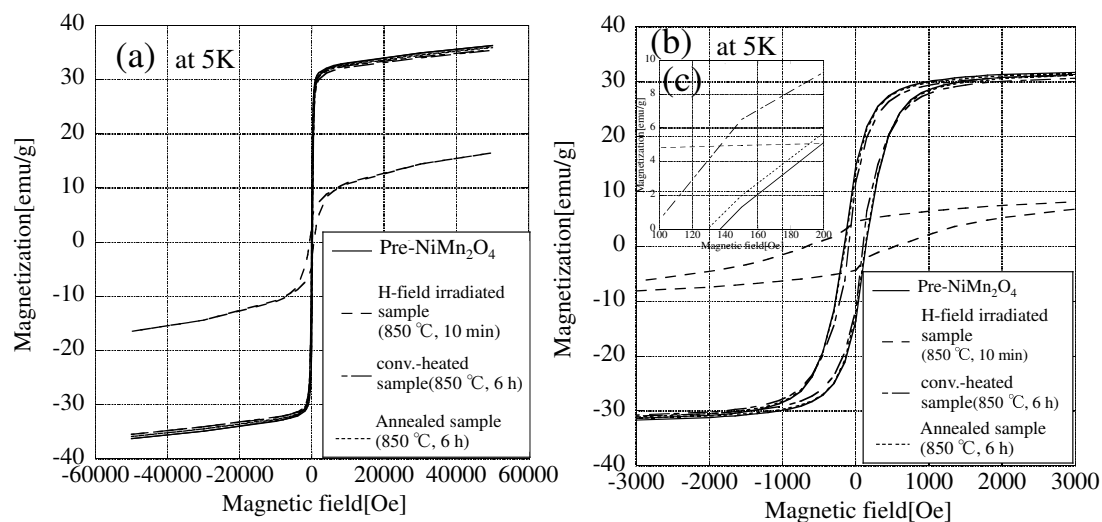


Figure 4. M-H loops at 5 K of NiMn₂O₄. (a) Full loop, (b) magnification (−3000–3000 Oe); and (c) magnification (100–200 Oe).

Table 1. Magnetic properties of synthesized NiMn₂O₄.

	Magnetization (emu/g) (at 50000 Oe)	Coercivity (Oe)
Pre-NiMn ₂ O ₄	36.3 ± 1.8	140 ± 7
H-field irradiated sample	16.5 ± 0.8	530 ± 27
conv.-heated sample	35.5 ± 1.8	95 ± 5
Annealed sample	36.0 ± 1.8	130 ± 7

The conv.-heated sample has almost the same saturation magnetization as Pre-NiMn₂O₄. On the other hand, the saturation magnetization of the H-field-irradiated sample was decreased significantly (decrease of about 54%). From Figure 4b, the coercivity of Pre-NiMn₂O₄ was almost the same as that of the conv.-heated sample. Table 1 shows that the coercivity after conventional heating has slightly decreased. On the other hand, the coercivity of the H-field-irradiated sample was increased significantly (by a factor of about 3.8) in comparison with Pre-NiMn₂O₄. The hysteresis of the H-field-irradiated sample is similar to that of the Ar-treated NiMn₂O₄, reported by Lisboa-Filho *et al.* [16]. Figure 5 shows zero-field-cooling and field-cooling (ZFC-FC) curves of Pre-NiMn₂O₄ and the H-field-irradiated sample.

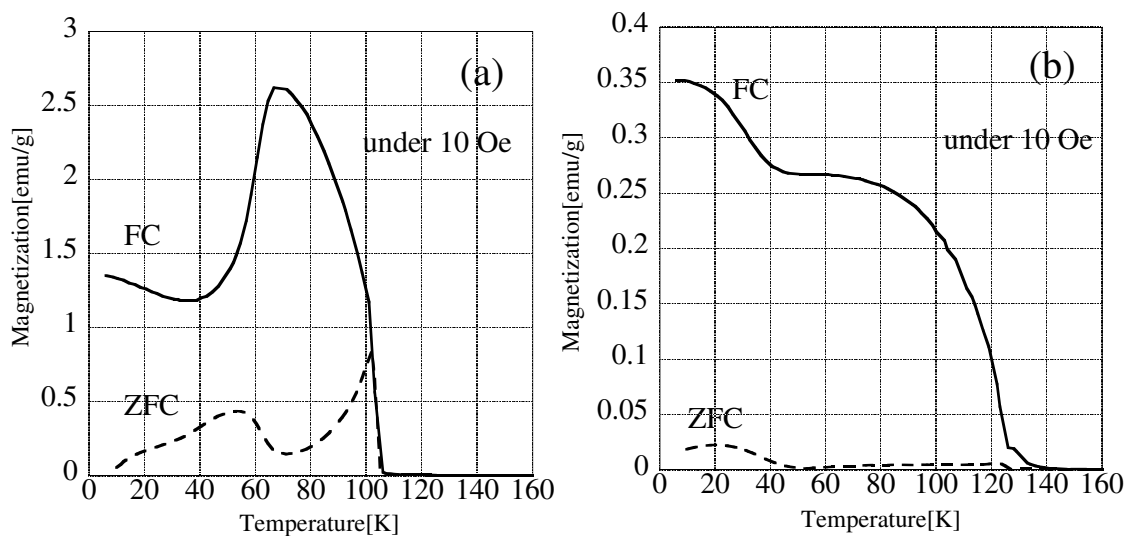


Figure 5. ZFC-FC curves of NiMn₂O₄. (a) Pre-NiMn₂O₄ and (b) H-field-irradiated sample (850 °C, 10 min).

The ZFC curve of Pre-NiMn₂O₄ has two magnetization peaks. Previously, it has been reported that NiMn₂O₄ is not a simple ferromagnet, but a unique magnet that has ferromagnetic and antiferromagnetic sublattices [16,28,29]. The exchange between Ni²⁺ and Mn³⁺ has antiferromagnetic character and the exchange between Mn²⁺ and Mn³⁺ has ferromagnetic character. This magnetic structure is caused by strong coupling between A-B sites [30]. When Mn²⁺ is created through reduction reaction, the Mn²⁺ ion will be adopted to tetrahedral site because of the large excess octahedral stabilization of Mn³⁺ [31]. From Figure 5, the contribution of sublattice was decreased. It is suggested that the contribution of super exchange interaction between Mn³⁺-O²⁻-Ni²⁺ (A-B interaction) became weak because Mn²⁺, which is adopted to tetrahedral site, was increased through the reduction of Mn³⁺ by microwave irradiation. The magnetic moments of the B sites are arranged into triangular configurations, which have canted-moment phases at low temperatures [15]. Judging from the ZFC-FC curve of Pre-NiMn₂O₄, the sample has a canted-moment magnetic structure below *ca.* 40 K and a collinear magnetic structure between 40 and 125 K. On the other hand, the ZFC-FC curve of H-field-irradiated sample shows no evidence for antiferromagnetic behavior and the magnetization decreases in two steps as the temperature increases. This change suggests

the loss of the canted-moment phase. In addition, ZFC-FC curves obtained under 1000 Oe of H-field-irradiated sample, Annealed sample and conv.-heated sample are shown in Supplementary material 2. The figure showed that the magnetization contributed from antiferromagnetic and ferromagnetic sublattice in H-field irradiated sample was significantly decreased compared to Annealed sample and conv.-heated sample. As ZFC-FC curves of Annealed sample and conv.-heated sample were almost the same, it is suggested that Mn^{2+} included in H-field irradiated sample was oxidized by annealing and the magnetic sublattice after annealing became to a similar sublattice of conv.-heated sample.

Previous studies have shown that the M-H loop and the ZFC-FC curve of NiMn_2O_4 were changed because of changing in the superexchange interaction and in the magnetic sublattice upon partial reduction of Mn^{3+} to Mn^{2+} [16]. A change in the magnetism in this experiment is also caused by partial reduction of Mn^{3+} to Mn^{2+} , because the M-H loop and the ZFC-FC curve are similar to the previously reported data [16]. The change in the magnetism in this experiment can be explained by the partial reduction of Mn^{3+} to Mn^{2+} in $\text{NiMn}_2\text{O}_{4-x}$ by the microwave H-field's enhancement effect on the reduction reaction. On the other hand, the magnetic properties of the conv.-heated sample are similar to those of Pre- NiMn_2O_4 . The results suggest that the effect of thermal reduction under air is small and that the superexchange interaction has not changed. Therefore, thermal reduction does not contribute at all to the reduction reaction; oxygen vacancies are produced by microwave H-field irradiation.

3.3. Effect of Annealing after Microwave Irradiation

To find out whether oxygen vacancies in the H-field-irradiated sample cause the changes in the magnetic properties, the microwave-irradiated sample was annealed under air using an electric furnace (Annealed-sample). Its XRD pattern was the same as that of the other samples. M-H loops of the Annealed-sample are shown in Figure 4. The saturation magnetization and coercivity of the Annealed-sample are the same as those of Pre- NiMn_2O_4 . This is because of a decrease in the number of oxygen vacancies upon annealing using an electric furnace under air. Figure 6 shows the ESR spectra of all samples.

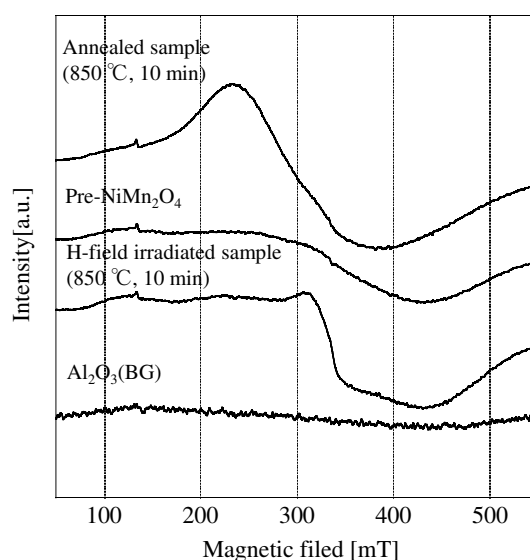


Figure 6. Electron spin resonance (ESR) spectra of NiMn_2O_4 .

Only the spectrum of the H-field-irradiated sample has a peak around 310 mT. NiMn_2O_4 generally only contains Mn^{3+} , which is ESR silent, Mn^{2+} and Mn^{4+} . However, ESR spectra of Pre- NiMn_2O_4 did not have clear peaks. Thus the amount of the Mn^{2+} and Mn^{4+} in Pre- NiMn_2O_4

was not large enough to appear in the ESR peaks. Annealed sample has a broad peak around 250 mT. In previous work, the peaks at 150–200 mT and around 250 mT were assign to Mn^{4+} and the peak at 300–400 mT was assign to Mn^{2+} and Mn^{4+} [32]. In H-field irradiated sample, the peaks at 150–200 mT and around 250 mT did not appeared, and the peak around 310 mT suggests the presence Mn^{2+} .

3.4. Controlling the Magnetic Properties of $NiMn_2O_4$ by a Microwave H-Field at Different Temperatures

M-H loops of microwave-irradiated $NiMn_2O_4$ (irradiated at different temperatures) are shown in Figure 7 and magnetic properties of the samples are listed in Table 2.

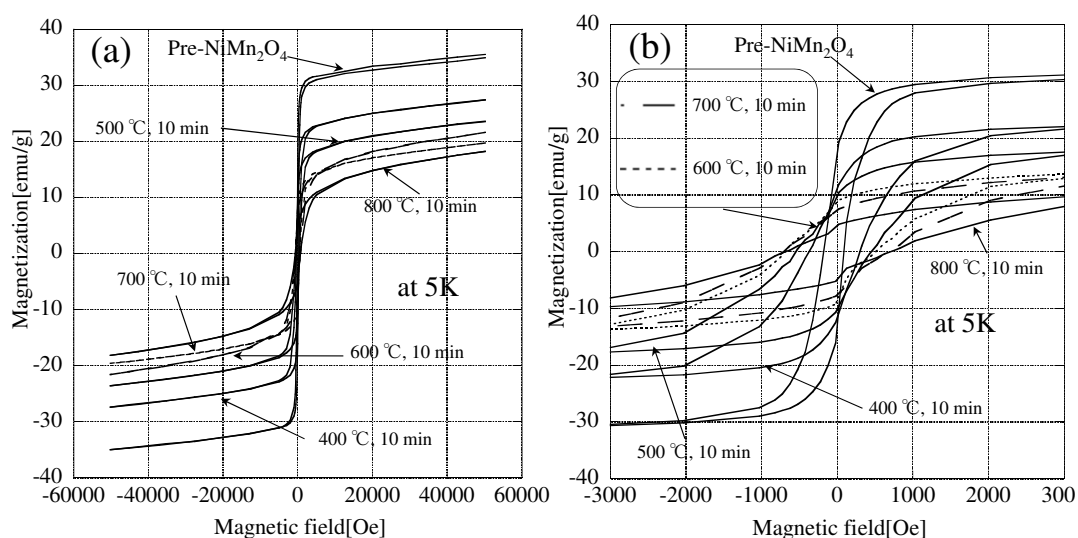


Figure 7. M-H loops of $NiMn_2O_4$ irradiated with a microwave H-field at different temperatures. (a) Full loops and (b) magnification (−3000–3000 Oe).

Table 2. Magnetic properties of $NiMn_2O_4$ irradiated with microwave H-field at different temperature.

	Magnetization (emu/g) (at 50000 Oe)	Coercivity (Oe)
Pre- $NiMn_2O_4$	35.3	140
H-field irradiated sample(400 °C)	27.4 ± 1.4	280 ± 14
H-field irradiated sample(500 °C)	23.5 ± 1.2	480 ± 24
H-field irradiated sample(600 °C)	19.7 ± 1.0	630 ± 32
H-field irradiated sample(700 °C)	21.6 ± 1.1	750 ± 38
H-field irradiated sample(800 °C)	18.2 ± 0.9	750 ± 38

These results show that a higher processing temperature results in a decrease in the magnetization and an increase in the coercivity. Furthermore, it can be seen that the emission of oxygen starts at a relatively low temperature (400 °C). Hence, we can control the nonstoichiometry and magnetic properties of $NiMn_2O_4$ by microwave H-field irradiation at different temperatures.

4. Conclusions

$NiMn_2O_4$ irradiated with microwave at the point of maximum H-field has a lower magnetization and a higher coercivity than the sample conventionally heated using an electric furnace. After annealing under air with an electric furnace, the magnetic properties are recovered to the state before microwave H-field irradiation. Although antiferromagnetic and ferromagnetic sublattices were confirmed by ZFC-FC curves of the presynthesized sample, only a ferromagnetic sublattice was confirmed after microwave H-field irradiation. Only the sample irradiated with microwave H-field shows a Mn^{2+} -derived peak in the ESR spectrum, which suggests that Mn^{3+} is partially

reduced. We can change the magnetic properties of NiMn_2O_4 by microwave H-field irradiation by manipulating the sample temperature. The above-mentioned effects are likely to be due to the microwave H-field's enhancement effect on the reduction reaction. By using microwave H-field irradiation, the stoichiometry of NiMn_2O_4 is controlled, which results in control over its magnetic properties. The microwave method for controlling stoichiometry could provide a new route to functional (magnetic, conducting, semiconducting, etc.) materials.

Supplementary Materials: The following are available online at www.mdpi.com/1996-1944/9/3/169/s1.

Acknowledgments: The authors would like to thank the Center for Low Temperature Science for assistance with the SQUID measurements and the Technical Division, School of Engineering, Tohoku University for assistance with ESR and TEM measurements. This work was supported by JSPS KAKENHI Grant Number 15K141150.

Author Contributions: Hiroshi Goto performed experiments, analyzed data and wrote the paper; Jun Fukushima designed experiments and wrote the paper; Hirotosugu Takizawa supervised its experiment and edited the manuscript.

Conflicts of Interest: The authors declare no conflict of interest.

References

1. Tsujimoto, Y.; Tassel, C.; Hayashi, N.; Watanabe, T.; Kageyama, H.; Yoshimura, K.; Takano, M.; Ceretti, M.; Ritter, C.; Paulus, W. Infinite-layer iron oxide with a square-planar coordination. *Nature* **2007**, *450*, 1062–1065.
2. Kageyama, H.; Watanabe, T.; Tsujimoto, Y.; Kitada, A.; Sumida, Y.; Kanamori, K.; Yoshimura, K.; Hayashi, N.; Muranaka, S.; Takano, M.; et al. Spin-ladder iron oxide: $\text{Sr}_3\text{Fe}_2\text{O}_5$. *Angew. Chem. Int. Ed. Engl.* **2008**, *47*, 5740–5745.
3. Hayward, M.A.; Green, M.A.; Rosseinsky, M.J.; Sloan, J. Sodium Hydride as a Powerful Reducing Agent for Topotactic Oxide Deintercalation: Synthesis and Characterization of the Nickel (I) Oxide LaNiO_2 . *J. Am. Chem. Soc.* **1999**, *121*, 8843–8854.
4. Overton, A.J.; Best, J.L.; Saratovsky, I.; Hayward, M.A. Influence of topotactic reduction on the structure and magnetism of the multiferroic YMnO_3 . *Chem. Mater.* **2009**, *21*, 4940–4948.
5. Hayward, M.A.; Cussen, E.J.; Claridge, J.B.; Bieringer, M.; Rosseinsky, M.J.; Kiely, C.J.; Blundell, S.J.; Marshall, I.M.; Pratt, F.L. The Hydride Anion in an Extended Transition Metal Oxide Array: $\text{LaSrCoO}_3\text{H}_{0.7}$. *Science* **2002**, *295*, 1882–1884.
6. Lindemer, T.B.; Hunley, J.F.; Gates, J.E.; Sutton, A.L.F.; Brynstad, J.; Hubbard, C.R.; Gallagher, P.K. Experimental and Thermodynamic Study of Nonstoichiometry in $\text{YBa}_2\text{Cu}_3\text{O}_{7-x}$. *J. Am. Ceram. Soc.* **1989**, *72*, 1775–1788.
7. Miyoshi, S.; Hong, J.O.; Yashiro, K.; Kaimai, A.; Nigara, Y.; Kawamura, K.; Kawada, T.; Kawada, J. Lattice expansion upon reduction of perovskite-type LaMnO_3 with oxygen-deficit nonstoichiometry. *Solid State Ion.* **2003**, *161*, 209–217.
8. Mizusaki, J.; Yoshihiro, M.; Yamauchi, S.; Fueki, K. Nonstoichiometry and Defect Structure of the Perovskite-Type Oxides $\text{La}_{1-x}\text{Sr}_x\text{FeO}_{3-d}$. *J. Solid State Chem.* **1985**, *58*, 257–266.
9. Uusi-Esko, K.; Rautama, E.L.; Laitinen, M.; Sajavaara, T.; Karppinen, M. Control of Oxygen Nonstoichiometry and Magnetic Property of MnCo_2O_4 Thin Films Grown by Atomic Layer Deposition. *Chem. Mater.* **2010**, *22*, 6297–6300.
10. Feteira, A. Negative temperature coefficient resistance (NTCR) ceramic thermistors: An industrial perspective. *J. Am. Ceram. Soc.* **2009**, *92*, 967–983.
11. Mehandjiev, D.; Zhecheva, E.; Ivanov, G.; Ioncheva, R. Preparation and catalytic activity of nickel-manganese oxide catalysts with an ilmenite-type structure in the reactions of complete oxidation of hydrocarbons. *Appl. Catal. A* **1998**, *167*, 277–282.
12. Mehandjiev, D.; Naydenov, A.; Ivanov, G. Ozone decomposition, benzene and CO oxidation over NiMnO_3 -ilmenite and NiMn_2O_4 -spinel catalysts. *Appl. Catal. A* **2001**, *206*, 13–18.
13. Hosseini, S.A.; Niaei, A.; Salari, D.; Nabavi, S.R. Nanocrystalline AMn_2O_4 (A=Co, Ni, Cu) spinels for remediation of volatile organic compounds-synthesis, characterization and catalytic performance. *Ceram. Int.* **2012**, *38*, 1655–1661.

14. Nelson-Cheeseman, B.B.; Chopdekar, R.V.; Alldredge, L.M.B.; Bettinger, J.S.; Arenholz, E.; Suzuki, Y. Probing the role of the barrier layer in magnetic tunnel junction transport. *Phys. Rev. B* **2007**, *76*, doi:10.1103/PhysRevB.76.220410.
15. Nelson-Cheeseman, B.B.; Chopdekar, R. V.; Iwata, J.M.; Toney, M.F.; Arenholz, E.; Suzuki, Y. Modified magnetic ground state in NiMn₂O₄ thin films. *Phys. Rev. B* **2010**, *82*, doi:10.1103/PhysRevB.82.144419.
16. Lisboa-Filho, P.N.; Bahout, M.; Barahona, P.; Moure, C.; Peña, O. Oxygen stoichiometry effects in spinel-type NiMn₂O_{4-δ} samples. *J. Phys. Chem. Solids* **2005**, *66*, 1206–1212.
17. Tadic, M.; Savic, S.M.; Jaglicic, Z.; Vojisavljevic, K.; Radojkovic, A.; Prsic, S.; Nikolic, D. Magnetic properties of NiMn₂O_{4-δ} (nickel manganite): Multiple magnetic phase transitions and exchange bias effect. *J. Alloy. Compd.* **2014**, *588*, 465–469.
18. Fukushima, J.; Kashimura, K.; Takayama, S.; Sato, M. Microwave-Energy Distribution for Reduction and Decrystallization of Titanium Oxides. *Chem. Lett.* **2012**, *41*, 39–41.
19. Fukushima, J.; Kashimura, K.; Takayama, S.; Sato, M.; Sano, S.; Hayashi, Y.; Takizawa, H. *In-situ* kinetic study on non-thermal reduction reaction of CuO during microwave heating. *Mater. Lett.* **2013**, *91*, 252–254.
20. Fukushima, J.; Sato, M.; Nakamura, H. Plasma Model for Energy Transformation Mechanism of Non-Thermal Microwave Effect. *Plasma Fusion Res.* **2012**, *7*, 1–2.
21. Kashimura, K.; Nagata, K.; Sato, M. Concept of Furnace for Metal Refining by Microwave Heating—A Design of Microwave Smelting Furnace with Low CO₂ Emission. *Mater. Trans.* **2010**, *51*, 1847–1853.
22. Kashimura, K.; Sato, M.; Hotta, M.; Agrawal, D.; Nagata, K.; Hayashi, M.; Mitani, T.; Shinohara, N. Iron production from Fe₃O₄ and graphite by applying 915MHz microwaves. *Mater. Sci. Eng. A* **2012**, *556*, 977–979.
23. Nagata, K.; Sato, M.; Hara, K.; Hotta, T.; Kitamura, Y.; Hayashi, M.; Kashimura, K.; Mitani, T.; Fukushima, J. Microwave Blast Furnace and Its Refractories. *J. Tech. Assoc. Refract. Jpn.* **2014**, *34*, 66–73.
24. Roy, R.; Peelamedu, R.; Hurtt, L.; Cheng, J.; Agrawal, D. Definitive experimental evidence for Microwave Effects: Radically new effects of separated E and H fields, such as decrystallization of oxides in seconds. *Mater. Res. Innov.* **2002**, *6*, 128–140.
25. Takayama, S.; Fukushima, J.; Nishijo, J.; Saito, M.; Sano, S.; Sato, M. Sintering of Soft Magnetic Material under Microwave Magnetic Field. *Phys. Res. Int.* **2012**, *2014*, 1–4.
26. Kumar, P.; Juneja, J.K.; Prakash, C.; Singh, S.; Shukla, R.K.; Raina, K.K. High DC resistivity in microwave sintered Li_{0.49}Zn_{0.02}Mn_{0.06}Fe_{2.43}O₄ ferrites. *Ceram. Int.* **2014**, *40*, 2501–2504.
27. Wickham, D.G. Solid-Phase Equilibria in the System NiO-Mn₂O₃-O₂. *J. Inorg. Nucl. Chem.* **1964**, *26*, 1369–1377.
28. Shen, Y.; Nakayama, T.; Arai, M.; Yanagisawa, O.; Izumi, M. Magnetic phase transition and physical properties of spinel-type nickel manganese oxide. *J. Phys. Chem. Solids* **2002**, *63*, 947–950.
29. Savić, S.M.; Tadić, M.; Jagličić, Z.; Vojisavljević, K.; Mancić, L.; Branković, G. Structural, electrical and magnetic properties of nickel manganite obtained by a complex polymerization method. *Ceram. Int.* **2014**, *40*, 15515–15521.
30. Yafet, Y.; Kittel, C. Antiferromagnetic arrangements in ferrites. *Phys. Rev.* **1952**, *87*, 290–294.
31. Arroyo, R.; Cordoba, G.; Padilla, J.; Lara, V.H. Influence of manganese ions on the anatase-rutile phase transition of TiO₂ prepared by the sol-gel process. *Mater. Lett.* **2002**, *54*, 397–402.
32. Dunitz, J.D.; Orgel, L.E. Stereochemistry of ionic solids. *Adv. Inorg. Chem. Radiochem.* **1960**, *2*, 1–60.

